Journal of Sustainability Science and Management 2009 Volume 4 (2): 125-140

TIDALLY INDUCED CROSS – SHORE SAND – MUD TRANSPORT AND LONG-TERM BED-PROFILE EVOLUTION

MOHAMMAD FADHLI AHMAD[a] AND PING DONG[b]

[a]*Department of Engineering Science, Faculty of Science and Technology, Universiti Malaysia Terengganu, Malaysia.*
[b]*Professor of Coastal Engineering, Division of Civil Engineering, School of Engineering, Physics and Mathematics, College of Art, Science and Engineering, University of Dundee, Scotland, UK.*

** Corresponding author e-mail address: fadhlikustem@yahoo.co.uk or fadhli@umt.edu.my and p.dong@dundee.ac.uk*

Abstract: A one-dimensional numerical model based on the shallow-water equations, suspended-sediment transport formulae and bed-material conservation equation was developed in order to study the morphological behaviour of idealised hump bed under cross-shore tidal current. A series of tests were carried out for some benchmark problems, such as wave propagation and hump morphodynamics, to validate the numerical scheme. The system of hydrodynamic equations was solved using the finite-volume numerical scheme associated with approximate Roe's Riemann solver, a data-reconstruction and slope limiter. Hump beds consisting of sand/mud mixtures were examined. It was found that the predicted morphological behaviours of the hump beds under the cross-shore tidal current for a five year period show quite similar trends and the height of hump-profiles is reduced at the top and increased at both sides. Moreover, sand content of 40 percent produces the highest peak of hump-bed profile. This study shows that the amount of decreasing and increasing of bed-profile depends on the critical shear-stress and quantity of sand and mud in the sediments fraction.

KEYWORDS: Sediment transport, shallow-water equations, morphodynamic, approximate Roe's Riemann solver.

Introduction

Cross-shore sediment transport due to currents and waves is responsible for many coastal engineering problems. Despite the extensive research over the past decades, the process of the movement of this particular sediment and the associated beach changes over the long term are still poorly understood. Sediment transport depends on so called 'active forces' which determine whether the displacement of the sand particles is either seaward or landward. The sediments usually move seaward rapidly during episodic storm events but during milder sea conditions they move gradually landward. If the environmental forces are maintained as constant, the profile and cross-shore sediment transport would approach equilibrium and zero respectively.

Sediment transport at a point in the near-shore zone is a vector with both long-shore and cross-shore components. For a number of coastal engineering scenarios of considerable interest, the transport is usually dominated by either the long-shore or cross-shore component and this, in part, has led to a history of separate investigation efforts for each of these two components. The subject of total long-shore sediment transport has been studied for approximately five decades assuming cross-shore sediment transport is relatively small (Dean, 1995).

The role of cross-shore tidal currents or tidal waves is important to determine the morphological changes of the bed. The systematic study of the morphology of sandy bed is enormous but much less so for pure muddy bed. A number of systematic studies (Dyer, 1998, Kirby, 2000, and

Pritchard, 2003) have been conducted to determine which forms of external forcing are responsible for developing and maintaining the observed equilibrium morphologies for muddy bed. Recently, INTRMUD (Inter-tidal mud) project on inter-tidal mudflat funded by the European Commission has been carried out with the aim of clarifying the properties of the sediment, understanding the mechanisms by which it is transported, and determining how the flat morphology varies with factors such as the tidal regime and the sediment properties and supply.

In real life, sediment does not exist with a single fraction, such as sand or mud, but comprises sand and mud or even together with gravel. To find out the realistic behaviour of sediment for long periods of time, it is necessary to bridge the knowledge-gap in the sediment-transport prediction concerning sand and mud mixture. The aim of this study is to investigate the morphodynamics behaviour of hump sediment beds over an extended period of time. To achieve this aim, the specific objectives are as follows: (1) To develop a numerical scheme to study the long-term behaviour of sediment humps consisting of sand-mud mixture; and (2) To analyse the morphological behaviour of the humps under tidal currents and sediment properties.

Methods

To achieve the first objective, the implementation of numerical schemes were conducted to the shallow-water flow model decoupled from the sediment transport and bed-level evolution models. The Godunov approach associated with approximate Roe's scheme solver, a balance technique prior to the numerical solution, a data-reconstruction and slope-limiter were used and tested with a standard tidal-wave propagation problem. For the morphodynamics, the shallow-water model was decoupled with bed-evolution model and tested by using the same approach to determine the accuracy of the numerical scheme. Then, idealised situation of hump beds comprising sand –mud was adopted to investigate their long-term morphological behaviours. In this case, the suspended-sediment transport model was a coupled shallow-water model whereas bed evolution was solved separately. A forward-difference scheme was used to solve bed-level model to obtain the bed changes. A parameterisation study was conducted to gain insight in the physical process of the flow and sediment transport.

Set-up of process-based models

In general, coastal problems occur at areas of tidal inlets, river mouths, estuaries and bays where the processes of sediment transport are very complex. Process-based morphodynamic models are required to predict and analyse the changes in the bed levels. In the past decades, a wide range of models has been developed and implemented to provide engineering solutions of coastal problems (Roelvink, 2006). Basically, these models consist of a set of equations which describes the currents and/or waves, sediment transport and bed level. Additional, numerical problems may arise in predicting the long-term morphological changes as the morphological models have to be run for extended periods of time and numerical schemes for solving the equations have to be sufficiently accurate and robust.

A set-up of the process-based models is developed in this work as shown in Figure 1. The process-based models are based on the hydrodynamic model, the sediment-transport model and bed-evolution model together with simplifications and assumptions are discussed.

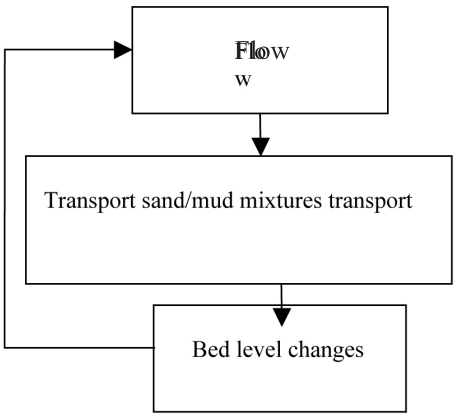

Figure 1. Model Set-up

Hydrodynamic model

In this study, a cross-shore tidal current was considered as the principal driving force for sediment transport. This assumption implies that the model is only applicable to areas which are protected from big waves by either man-made structures or natural obstructions. In the conservation of momentum equation (2), a bottom-stress model was included to represent the frictional effect of the bed on the flow. Other effects such as Coriolis, turbulent stresses, wind stress, atmospheric pressure at the water surface were ignored in the equation.

Under above assumptions, the mass and momentum conservation equations can be written as:

$$\frac{\partial h}{\partial t} + \frac{\partial (hu)}{\partial x} = 0. \tag{1}$$

$$\frac{\partial (hu)}{\partial t} + \frac{\partial \left(hu^2 + g\frac{h^2}{2} \right)}{\partial x} + gh\frac{\partial z_b}{\partial x} = \frac{-\tau_{bx}}{\rho} \tag{2}$$

where x = spatial coordinate; h = water depth; t = time; u = depth average velocity; z_b = bed elevation; g = gravity acceleration; ρ = water density;

$$\tau_{bx} = C_d u^2 \tag{3}$$

where τ_{bx} = bed shear stress and C_d = drag coefficient

Suspended sediment transport models

The one-dimensional concentration sediment transport without the diffusion term was implemented in this study assuming that the diffusion process was less significant than the advection process. Deposition experiments for sediment mixture of sand and mud particles showed that, if sediment concentrations in water column are low, the particles will behave independently from each other

(Torf, 1995). Therefore, the concentrations of sand and mud using the separate suspended-sediment transport equations for sand and mud fraction are given by

$$\frac{\partial}{\partial t}(hc_s)+\frac{\partial}{\partial x}(U_x hc_s)=E_s-D_s \quad (4)$$

$$\frac{\partial}{\partial t}(hc_m)+\frac{\partial}{\partial x}(U_x hc_m)=E_m-D_m \quad (5)$$

where h = total water depth; and U_x = depth average velocity in x-direction; c_s and c_m = sand and mud concentrations; D_s and D_m = sand and mud deposition, E_s and E_m = sand and mud erosion rates;

$$D_s = w_s c_s \quad (6)$$

$$D_m = w_m c_m\left[1-\frac{\tau_b}{\tau_d}\right] \quad (7)$$

where w_s = settling velocity for sand; w_m = settling velocity for mud;

$$E_s = (1-P_m)M_s\left[\frac{\tau_b}{\tau_{e,c}}-1\right] \quad (8)$$

$$E_m = P_m M_m\left[\frac{\tau_b}{\tau_{e,c}}-1\right] \quad (9)$$

where P_s = percentage of sand and P_m = percentage of mud; M_s = erosion rate for sand and M_m = erosion rate for mud; τ_b = bed shear-stress; τ_d = deposition shear-stress and $\tau_{e,c}$ = critical shear-stress.

The mud content P_m defined as the percentage of mud content in the bed sediments was included in the model. The mud content was assumed to be constant, thus, at every time step, when process of erosion occurs, the same proportion of sand and mud will be eroded and entrained into the water column.

Bed- level model

Since the bed in this study was assumed to be cohesive, the bed-load transport was ignored. The bed-level changes were modelled through the sediment budget equation which describes the evolution of the bed-level. For the cohesive sand and mud mixture, Van Ledden (2003) suggests the bed-level model can be described as

$$(1-\varepsilon_p)\frac{\partial z_b}{\partial t}=(D-E)_s+(D-E)_m \quad (10)$$

where s = sand fraction, m = mud fraction; ε_p = bed porosity and z_b = bed level.

In this work, the equation (10) was applied in simulations of sand-mud mixtures bed respectively. Bed porosity was assumed to be constant with time and space and takes a value of 0.4.

Morphological acceleration factor

The morphological acceleration factor (N) is a constant value used to assist in dealing with the difference in time-scales between hydrodynamic and morphological developments. It works by multiplying the changes in bed sediments by the morphological factor (N), thereby effectively extending the morphological time steps. It implies

$$\Delta t_{\text{morphological.}} = \text{N}\Delta t_{\text{hydrodynamic}} \tag{11}$$

The factor N simply increases the depth-change rates by a constant factor, so that after a simulation over one tidal-cycle, the morphology changes will be equivalent to that over N cycles. According to Roelvink (2005), this technique has an advantage because it is easy to include various interactions between flow, sediment and morphology and also removes the need to store large amounts of data between processes.

Numerical implementation - Godunov approach of finite-volume method

In this method, space was discretised into volumes, more often called cells, hence the general term of finite-volume method. The numerical solution is not characterised by its value at a set of points, but by its average over the cells. The evolution of the solution in a given cell is determined by the exchange (via fluxes) at the interfaces with all the neighbouring cells. In this approach, the fluxes are computed by solving Riemann problems at the interfaces between the cells.

To ensure the hydrodynamic results are correct in the simulation, the Godunov approach was used together with the Monotone Upstream-centred Scheme for Conservation Laws (MUSCL) and slope limiter. Furthermore a balance technique applied to the shallow water equations proposed by Roger et al. (2001) was also used.

Application of Roe's Riemann solvers, MUSCL and balancing of flux gradient and source terms

The Flux of Roe's Riemann Solver ia as follows:

$$F_{i+1/2} = \frac{F_L + F_R}{2} - \frac{1}{2}\sum_{p=1}^{m}(\tilde{\lambda}^{(p)}\ \tilde{\alpha}^{(p)}\ \tilde{K}^{(p)}) \tag{12}$$

where $\tilde{\alpha}^{(p)}$ = wave strength; $\tilde{\lambda}^{(p)}$ = eigenvalues; $\tilde{K}^{(p)}$ = right eigenvectors.

A new value of the conserve variable can be determined with the equation

$$U_i^{n+1} = U_i^n + \Delta t/\Delta x\left[F_{i-1/2} - F_{i+1/2}\right] \tag{13}$$

MUSCL can be obtained by reconstructing the data and a nonlinear slope-limiter version was used to prevent unphysical oscillations. This will render the scheme to total variation diminishing (TVD). Herein, the limiter was implemented such that, for consecutive cells i-1, i, i+1 on a locally uniform grid, the reconstructed Riemann states were given by

$$u_i^L = u_i(0) = u_i^n - \frac{1}{2}\Phi_i\Delta_{i-1/2};\quad u_i^R = u_i(\Delta x) = u_i^n + \frac{1}{2}\Phi_i\Delta_{i-1/2} \tag{14}$$

The slope limiter Φ_i proposed by Hirsch (1990) was used in the simulations. It is defined as

$$\Phi_i(r) = \max[0, \min(\beta r, 1), \min(r, \beta)] \tag{15}$$

where the limiter parameter $1 \le \beta \le 2$, and the gradient ratio is given by

$$r = \begin{Bmatrix} \dfrac{u_{i+1} - u_i}{u_i - u_{i-1}}, & u_i - u_{i-1} \neq 0, \\ 0 \qquad\quad , & u_i - u_{i-1} = 0 \end{Bmatrix} \tag{16}$$

The choice β 1.5 was used in the slope limiter.

Balancing of flux gradient and source term

A numerical imbalance is created by the artificial splitting of physical term $gh\dfrac{\partial \zeta}{\partial x}$ to give the flux gradients and source terms as (Roger et al., 2003)

$$gh\frac{\partial \zeta}{\partial x} = \frac{\partial}{\partial x}\left(\frac{1}{2}gh^2\right) + ghS_{ox} \tag{17}$$

(surface gradient term $\rightarrow$ flux gradient term + source term),

where g = gravitational acceleration; h = total water depth; ζ = water surface

S_{ox} = bed slope in x – direction.

According to Roger et al., (2003) the numerical difficulties arise with the splitting in the equation (17) if non-uniform bathymetries are accounted for such as in the case of wave propagation in this study. To avoid this problem, the technique suggested by Roger et al., (2003) was used.

The modified shallow-water equations in vector form are written as:

$$\frac{\partial}{\partial t}\begin{bmatrix} \zeta \\ uh \end{bmatrix} + \frac{\partial}{\partial x}\begin{bmatrix} uh \\ u^2 h + \dfrac{1}{2}g\left(\zeta^2 + 2\zeta h_s\right) \end{bmatrix} = \begin{bmatrix} 0 \\ -\left(gh\dfrac{\partial z_b}{\partial x} - gh_s\dfrac{\partial z_{b,s}}{\partial x}\right) \end{bmatrix} \tag{18}$$

For system 2 by 2 matrices, the Roe-averaged values for conserved variables in the Jacobian matrix, eigenvalues and corresponding right eigenvectors are

$$A = \begin{bmatrix} 0 & 1 \\ a^2 - \tilde{u}^2 & 2\tilde{u} \end{bmatrix};\ \lambda_1 = \tilde{u} - a,\ \ \lambda_2 = \tilde{u} + a;\ \ K^1 = \begin{bmatrix} 1 \\ \tilde{u} - a \end{bmatrix},\ K^2 = \begin{bmatrix} 1 \\ \tilde{u} + a \end{bmatrix} \tag{19}$$

where

$$\tilde{u} = \frac{u^R\sqrt{h^R} + u^L\sqrt{h^L}}{\sqrt{h^R} + \sqrt{h^L}};\ a = \sqrt{g\frac{h^R + h^L}{2}} \tag{20}$$

where subscript R and L are the right and left states of variable; and g = gravity acceleration

The wave strength $\tilde{\alpha}_1$ and $\tilde{\alpha}_2$ are given as

$$\tilde{\alpha}_1 = \frac{\Delta u_1\left(\tilde{u}+a\right)-\Delta u_2}{2a}, \quad \tilde{\alpha}_2 = \frac{-\Delta u_1\left(\tilde{u}-a\right)+\Delta u_2}{2a} \tag{21}$$

where $\Delta u_1 \equiv \zeta_R - \zeta_L$; $\Delta u_2 \equiv u_R h_R - u_L h_L$; (22)

For sand and mud mixture, the modified shallow-water equations and suspended-sediment transport are written in vector form as:

$$\frac{\partial}{\partial t}\begin{bmatrix}\zeta\\ hu\\ hc_m\\ hc_s\end{bmatrix}+\frac{\partial}{\partial x}\begin{bmatrix}hu\\ \left(u^2h+\frac{1}{2}g\left(\zeta^2+2\zeta h_s\right)\right)\\ huc_m\\ huc_s\end{bmatrix}=\begin{bmatrix}0\\ -\left(gh\frac{\partial z_b}{\partial x}-gh_s\frac{\partial z_{b,s}}{\partial x}\right)-C_d u^2\\ E_m-D_m\\ E_s-D_s\end{bmatrix} \tag{23}$$

where subscript *m* and *s* denote as mud and sand.

Eigenstructure in terms of conserved variables:

The Jacobian matrix (A), eigenvalues and eigenvectors are:

$$\mathrm{A}=\begin{bmatrix}0 & 1 & 0 & 0\\ a^2-\tilde{u}^2 & 2\tilde{u} & 0 & 0\\ -\tilde{u}\tilde{c}_m & \tilde{c}_m & \tilde{u} & 0\\ -\tilde{u}\tilde{c}_s & \tilde{c}_s & 0 & \tilde{u}\end{bmatrix} \quad \lambda_1=\tilde{u}-a;\ \lambda_2=\tilde{u}+a;\ \lambda_3=\tilde{u};\ \lambda_4=\tilde{u} \tag{24}$$

The wave strength of $\tilde{\alpha}_1$, $\tilde{\alpha}_2$, $\tilde{\alpha}_3$ and $\tilde{\alpha}_4$ are given as

$$\tilde{\alpha}_1=\frac{\Delta u_1\left(\tilde{u}+a\right)-\Delta u_2}{2a};\ \tilde{\alpha}_2=\frac{-\Delta u_3\left(\tilde{u}-a\right)+\Delta u_2}{2a}, \tag{25}$$

$$\tilde{\alpha}_3=\Delta u_3-\tilde{c}_m\Delta u_1;\ \tilde{\alpha}_4=\Delta u_4-\tilde{u}_s\Delta u_1$$

Discretisation for source term (S')

The source terms were evaluated in a pointwise manner and difference scheme was used to discretise the spatial gradients of bed elevation at node *i*.

$$S'=\begin{bmatrix}0\\ -\left(gh\frac{\partial z_b}{\partial x}-gh_s\frac{\partial z_{b,s}}{\partial x}\right)-C_d u^2\\ E_s-D_s\\ E_m-D_m\end{bmatrix}=\begin{bmatrix}0\\ -\frac{1}{\Delta x}(g)(z(i))\left(\frac{b(i+1)-b(i-1)}{2}\right)-C_d|u_i|u_i\\ \left(E_i-D_i\right)_s\\ \left(E_i-D_i\right)_m\end{bmatrix} \tag{26}$$

Discretisation for bed-evolution model

The bed-level model from equation (10) was applied to determine bed-level changes and an explicitly different scheme was used to discretise this equation. It is given as

$$z_b^{n+1} = z_b^n - \frac{1}{1-p}\Delta t\left[(D-E)_m + (D-E)_s\right]^t \tag{27}$$

Results and Discussion

Verification – Tidal-wave propagation with uneven bottom test problem

Bermudez & Vazquez (1994) discussed a tidal-wave propagation test problem that consists of the initial and boundary conditions as in Figure 2 and Figure 3 respectively.

$$\begin{aligned} h(x,0) &= 60.5 - B(x), \\ u(x,0) &= 0, \\ h(0,t) &= \begin{cases} 64.5 + 4\sin\left[\dfrac{\pi}{2}\left(\dfrac{t}{10800} - 1\right)\right] & , \text{if } t \le 43{,}200s \\ 60.5 & \text{if } t > 43200s \end{cases} \\ u(L,t) &= 0 \end{aligned} \tag{28}$$

and bathymetry

$$B(x) = \frac{40x}{L} + 10\left(1 - 10\sin\left[\pi\left(\frac{4x}{L} + \frac{1}{2}\right)\right]\right) \tag{29}$$

where L = 648,000m is the channel length. Under these conditions, the tidal wave of 4m amplitude enters the region at the upstream boundary (Figure 3). The tidal wave reaches a full height of 8m at t = 21,600s and since the wave propagates at approximately with $\sqrt{gh}$ then at t = 10,800s, the tidal wave can only reach as far as x = 216,000m for L = 648,000m. In this test problem, the bottom stress was not taken into account.

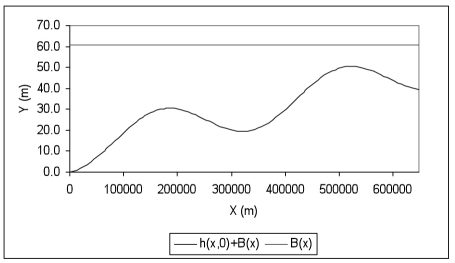

Figure 2. Initial condition

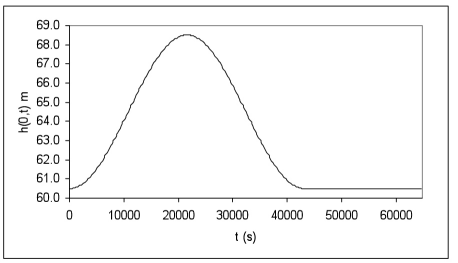

Figure 3. Upstream boundary condition

Numerical results

Figure 4 and Figure 5 illustrate the results of velocity (u) and surface elevation (h) after t=10800s using finite-volume numerical scheme respectively.

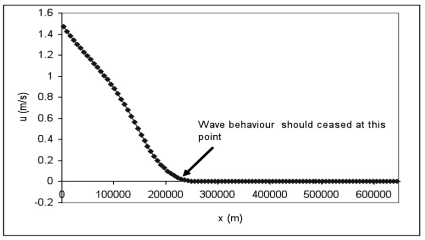

Figure 4. Velocity at t = 10800s

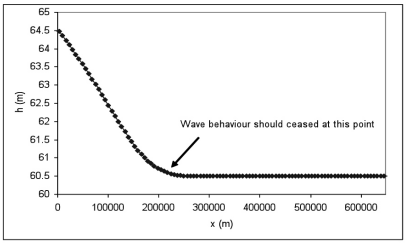

Figure 5. Water level at t = 10800s

The information of surface elevation (Figure 4) and velocity (Figure 5) are correct as expected at time 10800s. No waves propagate after the distance of 216000 m. From the figures, the Roe approximate Rieman solver produces good results when the shallow-water equation is balanced and the method of data reconstruction with slope-limiter is applied.

Verification – Morphodynamic of 1-D channel

To verify the morphodynamic changes using the mathematical balancing technique of Roger et al., (2003), 1-D channel problem (Hudson and Sweby, 2003) was selected. Test problem with B = 1m and Q = 10 is illustrated in Figure 6. The length of the channel is 1000m with the dummy initial conditions

$$h^*(x,0) = 10 - B(x,0) \text{ and } u^*(x,0) = \frac{Q_c}{h^*(x,0)}, \tag{30}$$

where Q_c = constant discharge; h^* = dummy water elevation; u^* = dummy velocity and B = bed elevation.

The initial bathymetry for the channel is shown as in Figure 6 and described by the equation as

$$B(x,0) = \begin{cases} \sin^2\left[\dfrac{\pi(x-300)}{200}\right], & \text{if } 300 \le x \le 500 \\ 0 & \text{otherwise} \end{cases} \tag{31}$$

To obtain the initial conditions, the water flow is iterated with the dummy initial conditions to an equilibrium state while keeping the bed fixed. The 1-D bed update equation (32) was used as

$$\frac{\partial B}{\partial t} + \xi \frac{\partial Q}{\partial x} = 0 \tag{32}$$

where $\xi = \dfrac{1}{1-\varepsilon}$, ξ, being the porosity of the bed, which is non-dimensional with $0 \le \varepsilon < 1$. The sediment-transport flux of Grass (1981) was used

$$Q(u) = Au|u|^{m-1} \tag{33}$$

where A is an empirical coefficient that encompasses the effects of grain size and kinematic viscosity. The m is chosen such that. $1 \le m \le 4$ In the present work, $\varepsilon = 0.4$ and $m = 3$ as recommended by Grass (1981) for bedload are used. Therefore it gives

$$Q(u) = Au^3 \tag{34}$$

The shallow-water equations and the bed-updating equation were numerically-integrated sequentially using the same time step. The water flow was calculated separately from the bed level.

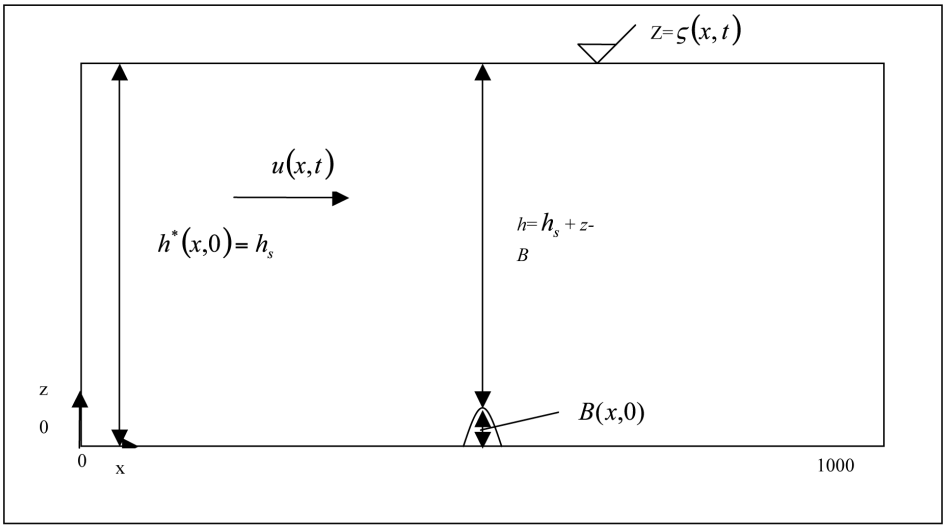

Figure 6. Bathymetry and coordinate system for the channel test problem

Numerical scheme

The shallow-water equations were solved as described before and the bed-updating equation, a Roe flux-limited version of Roe's scheme was used to discretise the formulation (Hudson and Sweby, 2003).

$$B_i^{n+1} = B_i^n - \frac{\Delta t}{\Delta x}\left(q^*_{i+1/2} - q^*_{i-1/2}\right) \tag{35}$$

where the numerical flux-function is

$$q^*_{i+1/2} = \frac{\xi}{2}\left(q^n_{i+1} + q^n_i\right) - \frac{1}{2}\left|\lambda^n_{i+1/2}\right|\left(1 - \phi\left(\theta^n_{i+1/2}\right)\right)\left(1 - \left|v^n_{i+1/2}\right|\right)\left(B^n_{i+1} - B^n_i\right) \tag{36}$$

with

$$v^n_{i+1/2} = \frac{\Delta t}{\Delta x}\left(\lambda^n_{i+1/2}\right), \quad \theta^n_{i+1/2} = \frac{B^n_{I+1} - B^n_I}{B^n_{i+1} - B^n_i}, \quad I = i - \mathrm{sgn}\left(v^n_{i+1/2}\right) \tag{37}$$

$$\phi\left(\theta^n_{i+1/2}\right) = \max\left(0, \min\left(1, \theta^n_{i+1/2}\right)\right) \tag{38}$$

$$\lambda_{i+1/2}^{n} = \xi\left[\frac{\partial q}{\partial B}\right]_{i+1/2}^{n} = \frac{A\xi mgu|u|^{m-1}}{gh-u^{2}} \tag{39}$$

To ensure the stability of the scheme, the time step was evaluated using

$$\Delta t = \frac{cf\,(\Delta x)}{\max\left(|u+c|\right)} \tag{40}$$

where cfl is the Courant number or Courant-Friedrichs-Lewy number and the cfl is less than 1.

Approximate solution

According to Hudson and Sweby (2003), by assuming the total height and the discharge of the channel are constant, then an approximate solution of the channel test problem can be achieved. The approximate solution is given as

$$B(x_0,t) = \begin{cases} \sin^2\left[\dfrac{\pi(x_0-300)}{200}\right], & \text{if } 300 \le x_0 \le 500 \\ 0 & \text{otherwise} \end{cases} \tag{41}$$

where the value of x is determined by substituting values of x_0 and t into

$$x = x_0 + A\xi m Q_c |Q_c|^{m-1} t \begin{cases} \left(D - \sin^2\left(\dfrac{\pi(x_0-300)}{200}\right)\right)^{-(m+1)} & \\ D^{-(m+1))} & \text{otherwise} \end{cases} \quad \text{if. } 300 \le x_0 \le 500 \tag{42}$$

Hudson and Sweby calculated the approximate solution for $m = 3$, $\varepsilon = 0.4$ and $Q_c = 10$ and identified the solution was only valid until the characteristics cross, which occurs at $t = 238079.124A^{-1}$ seconds in the region $300 \le x_0 \le 500$.

Numerical results

For the test case, a small hump on the bottom bed is interacting slowly with the water flow where A = 0.001 and Q_c = 10. Figure 7 illustrates the results obtained using the numerical scheme and approximate solution at $t = 238079$ seconds. To ensure the scheme is stable, $\Delta t = 0.1$ seconds and $\Delta x = 2.5$ m were chosen. As shown in Figure 7, the maximum difference between numerical scheme and approximate solution (Hudson and Sweby, 2003) is $7.7e^{-4}$ m for the bed bathymetry. The difference values, were obtained by deducting the approximation solution values and numerical values. From this result, the technique of balancing the flux gradient and source term was done before applying the numerical scheme to investigate the behaviour of sand-mud mixture bed.

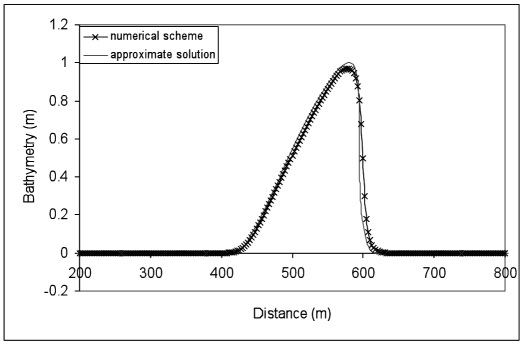

Figure 7. Comparison of the numerical scheme and approximate solution (Hudson and Sweby, 2003) with A = 0.001 and Q_c = 10 at t = 238079s.

Mudbank cases

Model set-up

An idealised situation to simulate the morphological behaviour is a mudbank as commonly found along the coast of North America. It has been reported that the sediment bed there consists of more than 95 percent of mud. According to Mehta (2002), such a mud bed can be consolidated under an appropriate combination of sediment supply and flow conditions. In this work, the mudbank consists of sand and mud mixture (cohesive).A consolidated mudbank was considered and sediment composition was assumed to be homogeneous for sediment mixture.

Geometry

A simplified geometry was used to represent the idealised situation as illustrated in Figure 8. The seaward end is located at point x = 0, and the landward end is located at point $x = L$, where the distance between these points is 10000 m. The consolidated sediment bed profile is flat with a half sinusoidal shape in the middle of the domain which visualises as a small hump. The hump with 1.0 m in height is submerged in the water of 20 m in height (h_o) . The bottom bed ($z = b_o$) is erodible and consists of cohesive sediments.

Boundary conditions

The water motion was generated by an external tidal motion at the sea side. Only the most important tidal component was considered in this study. It is given as

$$\zeta(t) = \zeta_0 \cos(\omega t) \tag{43}$$

where ζ = water level; ζ_0 = tidal amplitude; ω = tidal frequency = $\frac{2\pi}{T}$ where T = Time (taken as 12 hours).

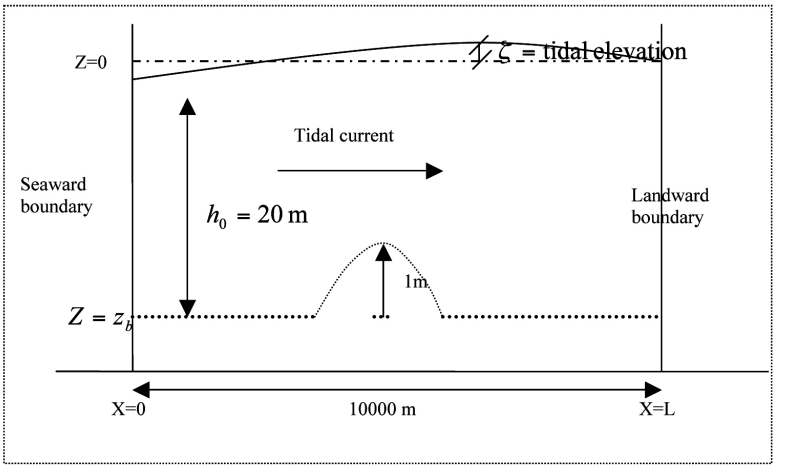

Figure 8. Model set-up of mud bank

Sediment concentration was not imposed at the sea boundary but it will occur when the process of erosion takes place on the bottom bed due to the excess bed-shear stress relative to critical bed-shear stress.

Physical parameters

The settings for the physical parameters depend on the case to be studied. Here, the bed was cohesive sand and mud mixture. The parameters are tabulated according to the cases as shown in the following sections. The parameters for sand and mud, such as the critical deposition τ_d and the settling velocity w_s, were set as constant within a realistic range. A quadratic drag law was used to express the bottom friction with coefficient C_d being taken as constant.

Numerical parameters

The horizontal grid size Δx was taken as 200 meter and time step Δt for the water motion, suspended-sediment transport and morphology was taken as 12 seconds. The time step in bed-level computation was multiplied by N, where N was the morphological factor and was taken to be 60. This morphological factor implies that for a simulation of 12 tidal cycles, it actually represents the morphological change over one year (Van Ledden, 2003).

Case 1 and case 2

For case 1, the settings for the physical parameters are tabulated in Table 1. It should be noted that the critical erosions for sand were set to different values for each test. Such settings were chosen to investigate the sensitivity of the model behaviour due to the critical erosion for sand and mud. The parameters for sand and mud, such as the critical shear-stress for deposition ($\tau_{c,d}$), the erosion rate (M_e), and settling velocity (w_s), were taken as similar for all tests. The percentage of mud and sand for all tests was taken as 90 % and 10 % respectively. For case 2, the settings for the physical parameters are tabulated in Table 2. It should be noted that the percentage of sand and mud were set to different values for each test. These tests investigated the sensitivity of the model behaviour due to proposition of sand and mud content. The parameters for sand, such as critical shear-stresses for

erosion ($\tau_{e,s}$), the critical shear-stress for deposition ($\tau_{d,s}$), the erosion rate (M_e), and settling velocity ($w_{s,s}$), were taken as similar for all tests. These parameters for the mud were also taken as similar for all tests. Fortran code was written to simulate the morphological behaviour for five years to determine the morphology behaviour.

Parameter	Test 1	Test 2	Test 3
Drag coefficient, C_d (dimensionless)	0.002	0.002	0.002
Constant rate erosion, M_e ($kg/m^2/s$)	0.000001	0.000001	0.000001
Critical erosion sand, $\tau_{e,s}$ (N/m^2)	0.20	0.25	0.20
Critical deposition sand, $\tau_{d,s}$ (N/m^2)	0.1	0.1	0.1
Settling velocity of sand, $w_{s,s}$ (m/s)	0.01	0.01	0.01
Percentage of sand, P_s (%)	10	10	10
Critical erosion mud, $\tau_{e,m}$ (N/m^2)	0.2	0.20	0.25
Critical deposition mud, $\tau_{d,m}$ (N/m^2)	0.15	0.15	0.15
Settling velocity of mud, $w_{s,m}$ (m/s)	0.005	0.005	0.005
Percentage of mud, P_m (%)	90	90	90
Tidal height, ζ (m)	1.1	1.1	1.1

Table 1. Parameters settings for sand and mud mixture (Case 1)

Parameter	Test 1	Test 2	Test 3
Drag coefficient, C_d (dimensionless)	0.002	0.002	0.002
Constant rate erosion, M_e ($kg/m^2/s$)	$1e^{-6}$	$1e^{-6}$	$1e^{-6}$
Critical erosion sand, $\tau_{e,s}$ (N/m^2)	0.25	0.25	0.25
Critical deposition sand, $\tau_{d,s}$ (N/m^2)	0.1	0.1	0.1
Settling velocity of sand, $w_{s,s}$ (m/s)	0.01	0.01	0.01
Percentage of sand, P_s (%)	0	25	40
Critical erosion mud, $\tau_{e,m}$ (N/m^2)	0.2	0.2	0.2
Critical deposition mud, $\tau_{d,m}$ (N/m^2)	0.15	0.15	0.15
Settling velocity of mud, $w_{s,m}$ (m/s)	0.005	0.005	0.005
Percentage of mud, P_m (%)	100	75	60
Tidal height, ζ (m)	1.1	1.1	1.1

Table 2. Parameters settings for sand and mud mixture (Case 2)

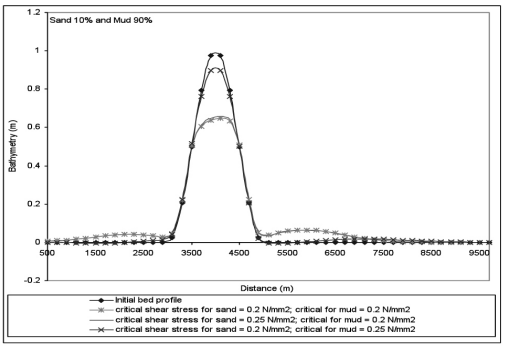

Figure 9. Bed profiles after 5 years (Case 1)

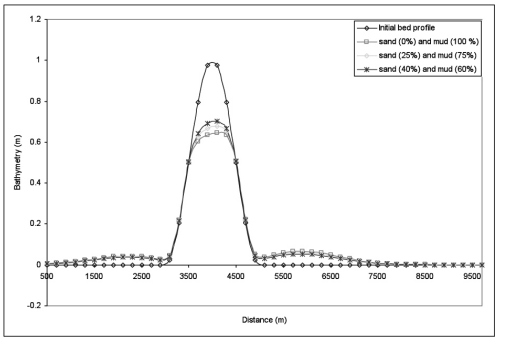

Figure 10. Bed profiles after 5 years (Case 2)

Results and Discussion

Figure 9 shows the results of calculated bed-profile with varying critical shear-stress of sand and mud. It can be seen that the critical shear-stress is an important parameter in determining the shape of the hump-profile. The shape is also influenced by the percentage of sediment fraction. In this case, the mud fraction is greater than the sand fraction so the mud fraction controls the behaviour of the hump with the critical shear-stress of 0.25 N/m^2 giving the highest hump-profile compared to the others. The critical shear stress for sand is less dominant in determining the shape due to less quantity of sand in the bottom beds. This figure also shows that the critical shear-stress for erosion of mud is very sensitive and can lead to a significant difference of predicted bed-profiles. This phenomenon implies that when the bed contains larger mud fraction than sand, the morphological changes are controlled by the critical shear-stress of mud rather than that of sand.

The Figure 10 illustrates the results of model calculations showing the effect of the sand adding to mud bed on the shape of the hump. It can be seen that general shape of the calculated profile is similar to that of case 1. It can also be seen that height of hump reduces as the percentage of sand adding to mud beds reduces. This means that the mud beds change its behaviour and becomes difficult to erode when the sand is added to it. This behaviour is consistent with the observations of Mitchener and Torfs (1996) who found that the critical shear stress for erosion increases when sand is added to mud beds or vice versa. Also from these results, it can be said that the proportion of the sand and mud fraction is important in determining the shape of the profile.

References

Bermudez, A. and Vazquez, M/E. (1994). 'Upwind methods for hyperbolic conservation laws with source terms, *Journal of Computers Fluids* , 23(8): 1049-1071.

Dean, R. G. (1995). *'Advances in coastal and ocean engineering'.* World Scientific.

Dyer, K.R. (1998). *'The typology of intertidal mudflats',* in K. Black et al., (eds.), Sediment Processes in the Intertidal Zone. London: Geo. Soc.

Grass, A.J. (1981). *Sediment transport by waves and current,* SERC London Cent. Mar. Technol, Report No. FL29.

Hirsch, H. (1990). *'Numerical computation of internal and external flows,* Vol. 2. Computational Methods for Inviscid and Viscous Flows. New York.

Hudson, J. and Sweby, P.K (2003). 'Formulations for numerically approximating hyperbolic systems governing sediment transport', *Journal of Science Computing,* 19: 225-252.

Kirby, R. (2000). 'Practical implications of tidal flat shape', *Journal of Continental Shelf Research,* 20:1061-1077.

Mehta, A.J. (2002). 'Mudshore dynamics and controls', in T. Healy, Y. Wang and J.A. Healy (eds.), Muddy coasts of the world: Processes, deposits and function, Proceedings in Marine Science, 4: 19-60.

Mitchener, H. and Torfs, H. (1996). 'Erosion of mud/sand mixtures', *Journal of Coastal Engineering,* 29: 1-25.

Pritchard, D. and Hogg, A. J. (2003). 'Cross-shore sediment transport and the equilibrium morphology of mudflats under tidal currents', *Journal of Geophysical Research,* 108(C10): 11(1-15).

Pritchard, D., Hogg A.J. and Roberts, W. (2002). 'Morphological modeling of intertidal mudflats: the role of cross-shore tidal currents', *Journal of Continental Shelf Research,* 22: 1887-1895.

Roberts, W., Hir, P. L. and Whitehouse, R.J.S. (2000). 'Investigation using simple mathematical models of the effects of tidal currents and waves on the profile shape of intertidal mudflats', *Journal of Continental Shelf Research,* 20: 1079-1097.

Roelvink, J.A. (2006) 'Coastal morphodynamic evolution techniques', *Journal of Coastal Engineering,* 53: 277-287.

Roger B. D., Fujihara, M. and Borthwick, A.G.L. (2001). 'Adaptive Q-tree Godunov-type scheme for shallow water equations', *International Journal for Numerical Methods in Fluids,* 35: 247-280.

Torfs, H. (1995). 'Erosion of sand/sand mixtures'. PhD. Thesis, Catholic University of Leuven, Leuven, Belgium.

Van Ledden, M. (2003). 'Sand and mud segregation'. PhD thesis, Delft University of Technology, Delft.